ORGANOMETALLICS

Article

pubs.acs.org/Organometallics

Synthesis, Air Stability, Photobleaching, and DFT Modeling of Blue Light Emitting Platinum CCC-N-Heterocyclic Carbene Pincer Complexes

Xiaofei Zhang,[†] Ashley M. Wright,[†] Nathan J. DeYonker,[‡] T. Keith Hollis,*[,†] Nathan I. Hammer,*[,†] Charles Edwin Webster,*[,‡] and Edward J. Valente[§]

[†]Department of Chemistry and Biochemistry, The University of Mississippi, University, Mississippi 38677, United States

[‡]Department of Chemistry, The University of Memphis, Memphis, Tennessee 38152, United States

[§]University of Portland Diffraction Facility, Department of Chemistry and Biochemistry, University of Portland, Portland, Oregon 97203, United States

Supporting Information

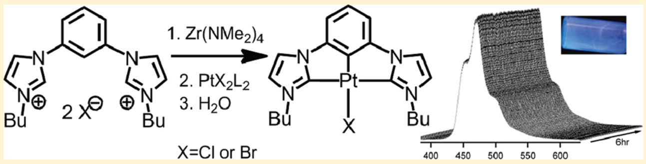

ABSTRACT: The recently reported metalation/transmetalation route for the synthesis of CCC-bis(NHC) pincer ligand supported transition-metal complexes was extended to Pt. 2-(1,3-Bis(*N*-butylimidazol-2-ylidene)phenylene)(chloro)-platinum(II) (**1**) and its bromo analogue **2** were synthesized and characterized. X-ray crystal structure determinations revealed complexes **1** and **2** to have distorted-square-planar configurations around the metal. Photophysical and thermal properties of these complexes are reported, and their extended photostability in air is discussed and contrasted. Density functional theory (DFT) and time-dependent density functional theory (TD-DFT) computations of the ground state and various low-lying excited states have revealed admixing of Pt 5d orbitals and the ligand π* orbitals for both the ground state and the low-lying excited states of complex **1**, indicating the low-lying states to be a mixture of metal-to-ligand charge-transfer and ligand-centered transition (MLCT-LC). Somewhat surprisingly, the computed gas-phase geometry of the excited state of complex **1** had a significant distortion, mostly about the C$_{aryl}$−Pt−Cl angle. These complexes were congeners of materials for organic light emitting diodes (OLEDs).

INTRODUCTION

The development of new molecular architectures to impart desired physical and chemical properties has been an area of highly active research. Specifically, stable carbenes have drawn intense attention, in spite of their relatively short history.[1] The special stability of N-heterocyclic carbenes (NHCs) was established with the first report of the X-ray crystallographically determined molecular structure by Arduengo and co-workers.[1b,2] The dramatic importance of the nitrogen substituents was further demonstrated when Alder and co-workers reported the X-ray crystal structure of an acyclic diamido carbene.[3] The applications of NHCs have blossomed since the 1991 report, and these compounds have been widely established as strong ligands for transition metals.[1c,4] Numerous applications to catalytic organic transformations have been demonstrated, including olefin metathesis,[5] Pd cross-coupling reactions such as the Heck,[6] Suzuki−Miyaura,[7] Negishi,[8] Sonogashira,[9] Buchwald−Hartwig,[7c,10] and many more.[11] In addition, they have been demonstrated to catalyze C−heteroatom bond forming reactions such as C−N,[10,12] C−Si,[13] and C−O.[14] Furthermore, their photophysical properties have been explored for materials applications.[15] Besides serving as excellent ligands to transition metals, NHCs have been demonstrated to be organocatalysts for the benzoin condensation,[16] Stetter reaction,[17] and more.[18]

Pincer ligands have been one of the most widely investigated and applied architectures in modern organometallic chemistry.[19] The confluence of NHCs and pincer ligand chemistry has seen much activity in recent years.[20] The aryl-bridged bis(NHC)-pincer ligands consist of four major classes, depending on the atoms making the bonds to the metal and the linker between the aryl and NHC groups (Scheme 1). The xylylene-bridged C^C^C-NHC (type A)[21] and 2,6-lutidinyl bridged C^N^C-NHC (type C)[20b,21c,22] pincer complexes are usually found to have C_2 symmetry due to the CH$_2$ spacer. The phenylene-bridged CCC-NHC (type B)[23] and pyridylene-bridged CNC-NHC (type D)[20b,c,24] pincer complexes normally have higher symmetry and adopt a C_{2v} geometry. We introduced the class of phenylene-bridged CCC-bis(NHC) pincer ligand systems,[23] and others have also begun exploring this architecture.[25]

The impact of molecular inorganic and organometallic compounds in photonic applications has been growing rapidly. Recent reports have illustrated their importance in developments for artificial photosynthesis,[26] photocatalytic splitting of water,[27] solar cell applications,[28] organic light-emitting diodes (OLEDs),[29] and photoluminescence.[15a,h,30] A recent paper detailed the pyridylene CNC-bis(NHC) pincer ligand Pt system

Received: August 2, 2011
Published: February 9, 2012

dx.doi.org/10.1021/om200687w | *Organometallics* 2012, 31, 1664−1672

Scheme 1. Metal Complexes Derived from Aryl-Bridged Bis(NHC)-Pincer Ligands

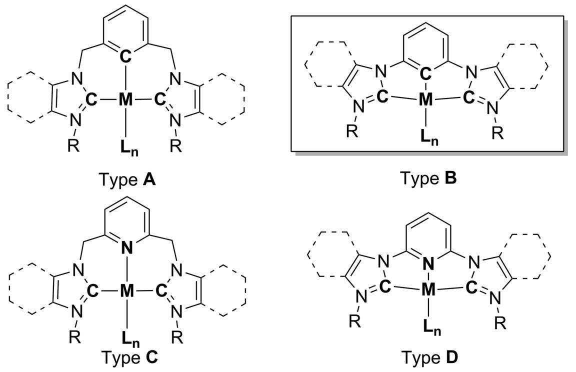

and its photoluminescence.[31] We report herein the development and characterization of square-planar Pt^{II} CCC-NHC phenylene-bridged pincer complexes **1** and **2** and their properties. To understand the nature of the observed transitions, we describe the application of theoretical methods (DFT) to explore the geometric and electronic properties of the ground state and excited state (both vertical and adiabatic transitions).

■ RESULT AND DISCUSSION

Synthesis and Characterization. The CCC-NHC pincer ligand precursors were synthesized according to the literature.[23,32] Simultaneous activation of the three C−H bonds of the tridentate ligand was achieved through the well-established basicity and electrophilicity of $Zr(NMe_2)_4$.[23,33] A Pt(II) source was added to the in situ prepared Zr reagent to achieve transmetalation (Scheme 2). All reactions were carried out at room temperature under an inert atmosphere. When transmetalation was complete, water was added, and excess Zr reagent was decomposed and precipitated. The identity of each complex was established by ^1H and ^{13}C NMR spectroscopy, ESI-MS, and elemental analysis (see the Experimental Section). Two of the primary observations in the ^1H NMR spectra were the disappearance of the imidazolium protons (11.27 ppm, 2H) and an aryl H (8.96 ppm). The ^1H NMR data of chloro complex **1** and bromo complex **2** also indicated characteristic long-range $^{195}Pt-^1H$ coupling. The NHC carbon signal of chloro complex **1** was observed at 171.7 ppm with $^1J_{Pt-C}$ = 1168 Hz. The Pt-bound aryl carbon signal was observed at 133.8 ppm with $^1J_{Pt-C}$ = 937 Hz. The NHC carbon signal of bromo complex **2** was observed at 170.5 ppm with $^1J_{Pt-C}$ = 1166 Hz. The Pt-bound aryl carbon signal of **2** was observed at 134.0 ppm with $^1J_{Pt-C}$ = 953 Hz. All chemical shifts and coupling constants were similar to those previously reported for Pt-NHC complexes.[31,34] The ESI-MS of the Pt-Cl complex **1** revealed the molecular ion plus Na (575 Da). The molecular ion was observed for the Pt-Br complex **2** (595 Da). The experimental values for the CHN analyses of both complexes were within an acceptable range.

Scheme 2. Synthesis of CCC^{Bu}-NHC-Pt^{II}-X Complexes 1 and 2

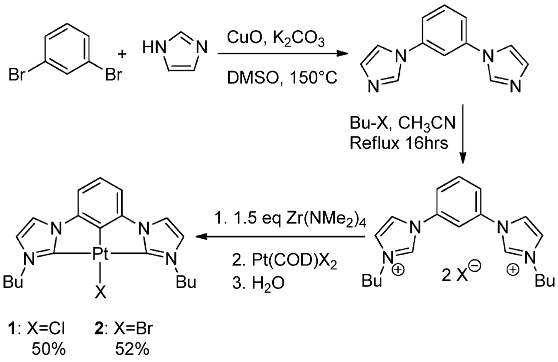

X-ray-quality crystals of chloro complex **1** were obtained by slow diffusion of Et_2O into a CH_2Cl_2 solution. X-ray-quality crystals of bromo complex **2** were observed after transmetalation and were collected from the reaction mixture. ORTEP representations of the molecular structures of **1** and **2** are depicted in Figure 1.[35] Selected bond distances and angles for complexes **1** and **2** are given in Table 1 and are consistent with those for previously reported Pt(II) complexes.[31,34a,36] The structural data for the pyridylene-bridged CNC analogue have been listed for comparison.[31] The structures of complexes **1** and **2** are similar. The Pt−C$_{carbene}$ bond distances in chloro complex **1** (2.030(3) and 2.035(3) Å) and in bromo complex **2** (2.037(6) and 2.036(6) Å) fall into the range observed for neutral and cationic Pt(II) pincer complexes.[31,34a,36] Both complexes display distorted-square-planar configurations at the metal center, which has been commonly seen for four-coordinate Pt(II) complexes.[34a,36] The C7−Pt^{II}−X atoms are linear (**1**, 179.40(8)°; **2**, 178.66(18)°). However, the C2−Pt^{II}−C13 angles were bent (**1**, 157.44(11)°; **2**, 157.3(2)°) due to ligand constraints.

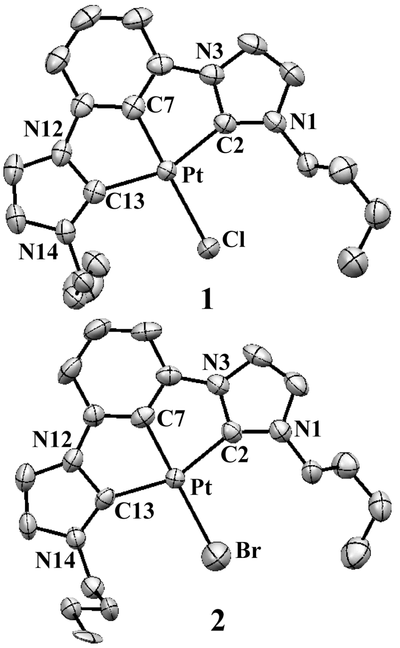

Figure 1. ORTEP diagram (50% thermal ellipsoids) of CCC^{Bu}-NHC-Pt^{II}-Cl (**1**) and CCC^{Bu}-NHC-Pt^{II}-Br (**2**). Hydrogen atoms are omitted for clarity.

It was possible to compare the metric data for Pt−Cl complex **1** to those for its pyridylene-bridged CNC analogue. The Pt−C$_{aryl}$ bond length of complex **1** (1.941(3) Å) was slightly shorter (~0.025 Å) than the Pt−N bond length of the pyridylene-bridged CNC complex, while the Pt−C$_{NHC}$ bonds of complex **1** were about 0.06 Å longer.[31] On comparison of the Pt−Cl bond distances, a greater trans influence of the C$_{aryl}$ anionic ligand was

Table 1. Selected Bond Lengths and Angles of CCC^{Bu}-NHC-Pt^{II}-X Complexes **1** (X = Cl) and **2** (X = Br) and the CNC^{Bu}-NHC-Pt^{II}-Cl Complex

	bond lengths (Å)				bond angles (deg)		
	Pt−C2	Pt−C7	Pt−C13	Pt−X	C7−Pt−X	C2−Pt−C13	C7−Pt−C2
1	2.030(3)	1.941(3)	2.035(3)	2.3997(7)	179.40(8)	157.44(11)	78.58(11)
2	2.037(6)	1.955(6)	2.036(6)	2.5028(8)	178.67(18)	157.3(2)	78.9(3)
	bond lengths (Å)				bond angles (deg)		
	Pt−C1	Pt−N1	Pt−C9	Pt−X	N1−Pt−Cl	C1−Pt−C9	N−Pt−C1
CNC[a]	1.972(8)	1.968(5)	1.978(9)	2.278(2)	178.79(18)	158.1(3)	79.1(3)

[a] Pyridylene-bridged CNC analogue with X = Cl. Data from ref 31.

notable in the longer bond length (2.3997(7) Å vs 2.278(2) Å, Table 1). Other metric data for the two compounds were very similar.

Photophysical Studies. Complexes **1** and **2** were found to emit blue light with UV stimulation. Their absorption and emission data in MeOH solution have been included in Table 2 and Figure 2a. In MeOH solution, the UV absorption spectra of complexes **1** and **2** were nearly identical. Both exhibited a major absorption peak around 265 nm and minor peaks near 323 and 355 nm, which were ascribed as mixed metal to ligand charge transfer and ligand centered (MLCT-LC) transitions.[37] The d−d transitions that lead to absorption peaks above 400 nm with significant strength were consistent with a distorted-square-planar configuration of each complex.[38] The emission spectra of complexes **1** and **2** were very similar, except for the ratio of major peaks (Figure 2a). Observed solution quantum efficiencies were 1.3% for complex **1** and 1.5% for complex **2** (Table 2). Lifetimes of excited states in methanol solutions were 210 ns for complex **1** and 1.7 μs for complex **2**, which was comparable to those for organometallic complexes with related structures.[15a]

Table 2. Photophysical Properties of CCC^{Bu}-NHC-Pt^{II}-X Complexes **1** and **2** in MeOH Solution

	λ_{abs}/nm (ε/10^{-3} M^{-1} cm^{-1})	λ_{em}/nm (rel intens)	Φ_{obs}/%	τ/μs
1	265 (22.9), 323 (3.3), 355 (5.7), 416 (0.12), 441 (0.08)	449 (100), 474 (63)[a]	1.3[b]	0.21
2	266 (24.0), 323 (3.5), 358 (6.2), 416 (0.13), 440 (0.08)	450 (100), 474 (77)[a]	1.5[b]	1.7

[a] Irradiated with 360 nm light. [b] Referenced to quinine sulfate.

In the solid state, the strong blue emission of complexes **1** and **2** varies only slightly (Figure 2b). While sharing λ_{max} at 472 nm, complex **2** had a more intense shoulder peak at 455 nm, which suggested a Pt to halogen interaction was involved in the emission process. The emission curves extended to about 600 nm, but the sharp drop after the peak at ~480 nm gave the complexes a pure blue color. In comparison to the pyridine-bridged analogue reported by Lee et al.,[31] complexes **1** and **2** gave relatively narrow emission peaks (half peak width of ~50 nm), and they were blue-shifted 100−150 nm. Decay of the excited state of complexes **1** and **2** in the solid state exhibited a biexponential pattern. The lifetimes of excited states of **1** (0.19 and 1.7 μs) and **2** (0.19 and 1.9 μs) are comparable to those of other known organometallic complexes.[15c,39] No difference in lifetime was observed between ambient and vacuum (10^{-5} Torr) conditions for the solid state.

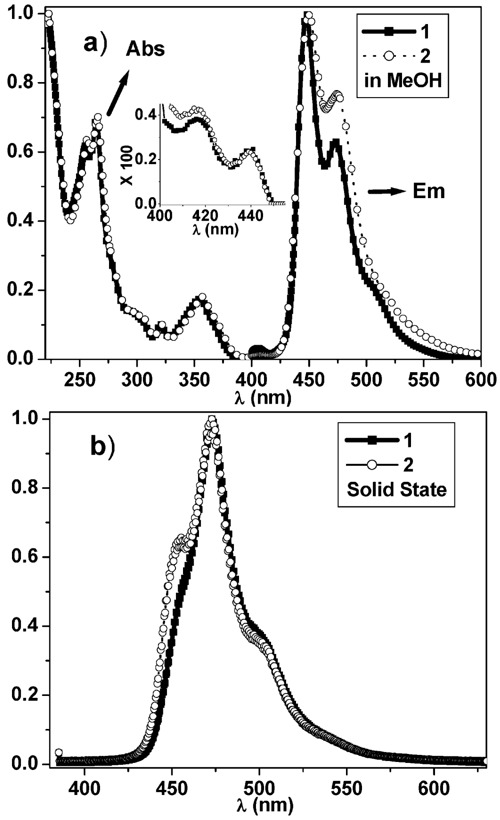

Figure 2. Emission and absorption data of CCC^{Bu}-NHC-Pt^{II}-X complexes **1** and **2** in (a) MeOH solution (the insert shows d−d transitions) and (b) solid state at 298 K (irradiated at 355 nm).

Thermophysical Studies. Thermal stability is crucial to OLED emitter candidates. The thermal properties of complexes **1** and **2** were investigated by thermogravimetric analysis (TGA) and differential scanning calorimetry (DSC). It was found that the compounds melted at approximately 280 °C and remained as supercooled liquids over a large temperature range. The 10% weight loss temperatures ($T_{\Delta 10\%}$) were about 380 °C (see the Supporting Information). Notably, complexes **1** and **2** evaporated and deposited on the glass wall of the furnace. Spectroscopic analysis of the residues (fluorescent, NMR, and ESI-MS) indicated the compounds remained unchanged.

Photostability in Air. Previous studies on Pt NHC complexes suggested that their emissions could be stable under an inert atmosphere over an extended period of time.[15c,40] Interestingly, the emissions of complexes **1** and **2** were found to be stable even under an ambient atmosphere (room temperature and 30−50% humidity). Time-resolved emission spectra of **1** and **2** are presented in Figure 3. The authentic blue λ_{max} (472 nm) of complexes **1** and **2** retained >97% intensity over 6 h of continuous irradiation. The shape of the spectra remained unvaried during the

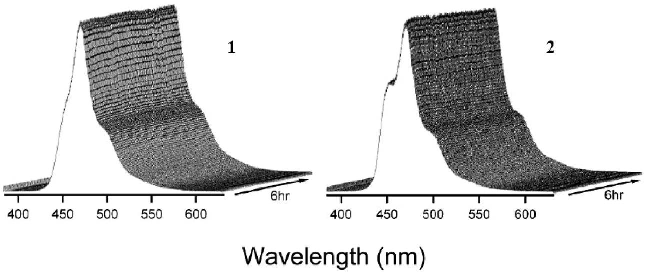

Figure 3. Time dependence of emission of solid-state **1** and **2** in air over 6 h, irradiated at 355 nm.

Table 3. Solid-State Emission and Lifetime Data of CCC^{Bu}-NHC-Pt^{II}-X Complexes 1 and 2 and Four Commercially Available Emitters

		remaining intens/%^{b}		$\tau_{obs}/\mu s$	
	λ_{em}/nm (rel intens/%)^{a}	in N_2	in air	in air	in vac
1	445 (39) 472 (100) 502 (42)		99 (0.4)	0.19/1.7	0.19/1.7
2	455 (66) 472 (100) 502 (33)		97 (0.3)	0.19/1.9	0.19/1.9
Alq$_3$	506 (100)	99 (0.2)	51 (3.8)	0.016^{c}	
Ir(dfppy)$_3$	499 (100)	71 (4.6)	46 (3.0)^{d}		
Znq$_2$	536 (100)	99 (1.8)	78 (1.8)	0.025^{e}	
LBMQ	463 (100)	99 (0.3)	84 (5.6)		

^{a}Irradiated at 355 nm (1.67 mW/cm^2). $^{b}\lambda_{max}$ after 6 h of continuous excitation. Data presented are an average of three measurements; σ (standard deviation) values are included in parentheses. ^{c}See ref 41, data collected under nitrogen. ^{d}After 1 h. ^{e}See ref 43, data collected under nitrogen.

measurements (Figure 3 and Table 3). These data indicated that complexes **1** and **2** did not photobleach in air with UV irradiation.

Scheme 3. Four Commercially Available Emitters

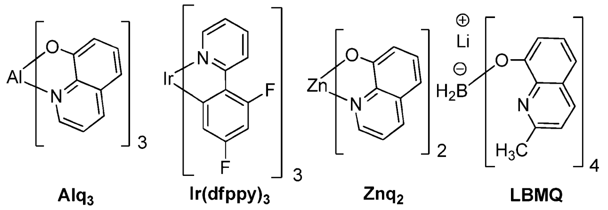

The photostability test under N_2 and ambient atmosphere was also carried out on four commercially available emitters: tris(8-hydroxyquinoline)aluminum (Alq$_3$),[29a,41] tris[2-(4,6-difluorophenyl)pyridinato-C^2,N]iridium(III) (Ir(dfppy)$_3$),[42] (8-hydroxyquinoline)zinc (Znq$_2$),[43] and lithium tetrakis(2-methyl-8-hydroxyquinolinato)boron (LBMQ)[44] (Scheme 3). Three of the emitters, Alq$_3$, Znq$_2$, and LBMQ, were found to be stable to photoexcitation under nitrogen (no significant loss of emission intensity after 6 h). Ir(dfppy)$_3$ showed significant loss of intensity of λ_{max} (29%) after 6 h of photoexcitation under the same conditions. When these commercially available complexes were irradiated under ambient atmosphere, moderate to severe photobleaching was observed. Ir(dfppy)$_3$ exhibited a loss of more than half of its initial emission strength and a visible darkening on the irradiated surface after only 1 h (Table 3). When significant photobleaching (>10%) was observed under any conditions, a control experiment was carried out to calibrate the contribution to decomposition from other pathways. In the control experiment, the initial emission spectrum A was collected and the analyte was then kept under the same conditions with the radiation beam blocked. After 1 h the irradiation was resumed and another emission spectrum B was taken. The loss of emission intensity between spectra A and B was ascribed to the sum of decompositions through all other pathways. Since each spectrum took ~2 min to accumulate, a significant measurement-induced photobleaching was observed for the less photostable analytes (Figures S1 and S2, Supporting Information). An exponential fitting based on the decay curve was applied to retrieve the photobleaching during the initial 2 min irradiation. After 1 h in the dark all compounds were found to undergo <1% decomposition, which confirms a direct correlation between photobleaching and loss of emission strength. On comparison of the pincer Pt(II) complexes **1** and **2** and the four commercially available emitters, these observations indicated that the Pt complexes were much more photostable under an ambient atmosphere.

Computational Studies. The pincer Pt(II) complexes were modeled by DFT and TD-DFT methods to better understand the observed photophysical properties.[45] Previously, Halls and Schlegel employed a somewhat similar approach to study the first excited states of tris(8-hydroxyquinoline)aluminum(III) (Alq$_3$).[46] Additionally, Rocha, Martin, Batista, and co-workers successfully used DFT/TD-DFT theoretical methods and experimental approaches to study the electronic structure and spectroscopic properties of ruthenium polypyridyl complexes.[47] In our calculations the structure of Pt-Cl complex **1** was simplified to structure **3** by replacing the two butyl groups with methyl groups. The computationally predicted ground-state geometry of **3** was in very good agreement with the geometric results from the experimental X-ray crystallography of **1**. The rms deviation of the 20 heavy atoms was 0.047 Å.

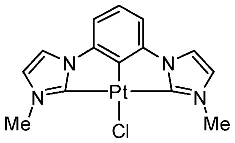

3

The absorbance and fluorescence spectra for CCC^{Me}-NHC-Pt^{II}-Cl (**3**) were computed using the optimized molecular structure (Figure 4). The simulated absorption of structure **3** matched the experimental data of complex **1** in the energy range (230−380 nm). However, the calculated emission spectrum of the optimized planar excited-state geometry was very different from the experimental result (compare Figure 2a vs Figure 4 (×)), indicating that the planar excited state of the molecule was not the major radiative state.

Further TD-DFT calculations revealed that although CCC^{Me}-NHC-Pt^{II}-Cl (**3**) adopts a distorted-square-planar configuration at the ground state, constraining the first singlet excited electronic state to the C_{2v} point group symmetry actually leads to a transition state. The imaginary vibrational mode (ω_e = 58.7i) corresponded to the Cl atom and the sides of the two pincer ligand asymmetrically bending out of the C_{2v} plane. When performing a TD-DFT geometry optimization of the first excited state in C_s symmetry, the Cl atom bent out of

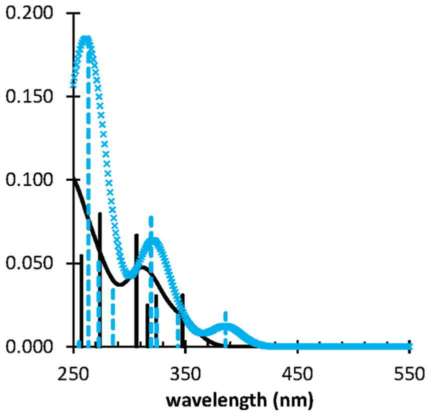

Figure 4. Computed ground state absorbance (−) and C_{2v} (planar) excited state emission (×) of CCC^{Me}-NHC-Pt^{II}-Cl (**3**).

plane significantly (C_{aryl}−Pt−Cl = 93°). HOMO and LUMO diagrams (Kohn−Sham orbitals) of the planar ground state and the optimized C_s-symmetric excited state are included in Figure 5. In the ground state, significant admixture among the d orbitals of Pt, the 3p orbital of Cl, and the ligand π orbital was observed in both the HOMO and LUMO (Figure 5a,b). In the excited state, the Cl atom bends out of the molecular plane along the C_{aryl}−Pt−Cl axis, leading to C_s symmetry (Figure 5c−f). The molecular orbitals are highly localized around the Pt and Cl atoms.

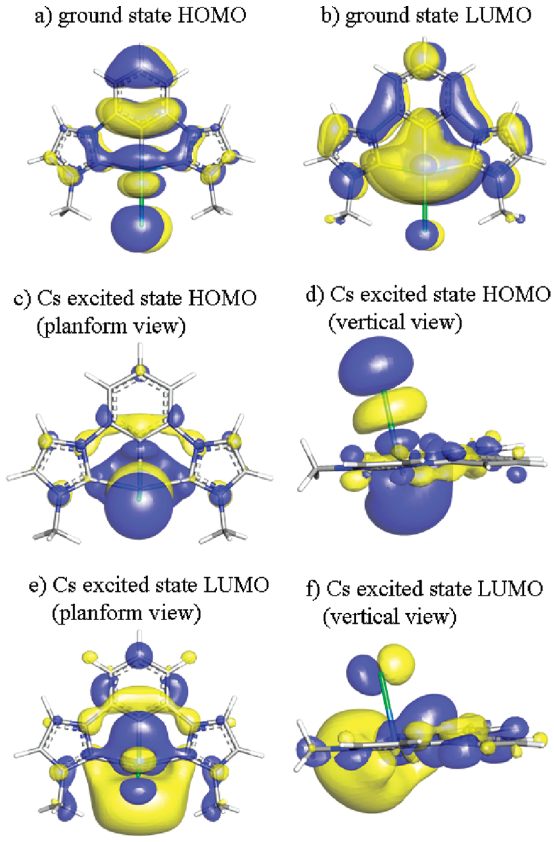

Figure 5. Molecular orbitals of the optimized ground state and optimized excited state of complex CCC^{Me}-NHC-Pt^{II}-Cl (**3**).

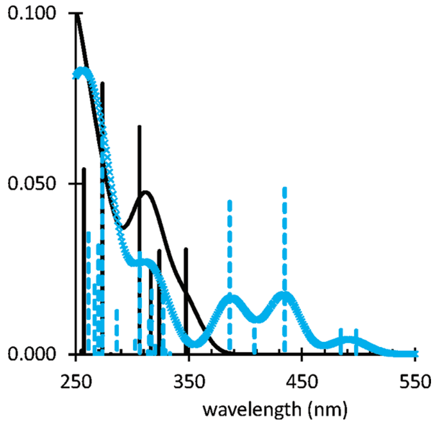

Figure 6. Computed ground state absorbance (−) and optimized C_s excited state emission (×) of CCC^{Me}-NHC-Pt^{II}-Cl (**3**).

An emission spectrum was calculated on the basis of the optimized C_s geometry for the bent singlet excited state (S_1). The S_1 emission spectrum (Figure 6 (×)) was much closer to the observed one (Figure 2). S_1 and the optimized C_s geometry for the bent triplet excited state (T_1) are quite similar.[48] The simulated spectrum suggested an emission from 380 to 510 nm with three major peaks at 390, 445, and 490 nm. This result matched the experimental data very well in the energy range and in having three maxima. The simulated absorbance spectrum is included in Figure 6. Compare the computed emission spectra of the planar C_{2v} and bent C_s structures—the computed emission spectrum of the planar structure has only a small red shift, while the computed emission spectrum of the distorted structure has a much larger red shift. In the bent C_s excited state, the HOMO−LUMO transition loses almost all of its intensity and moves to around 1200 nm (see the Supporting Information). Also, in the bent C_s excited state, the first transition with appreciable intensity in the visible region was the third computed singlet electronic excitation.

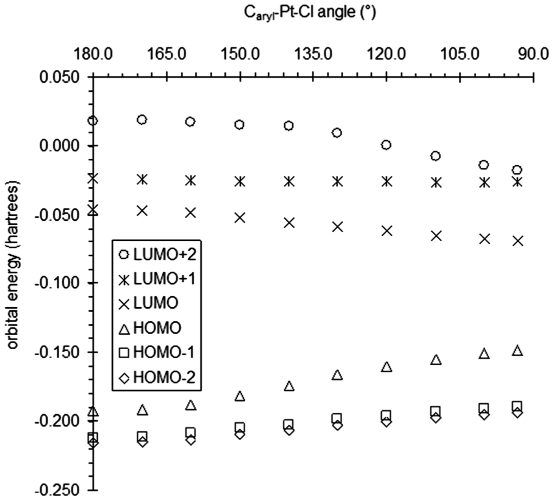

Figure 7. Walsh-like diagram of the ground-state orbital energies at the TD-DFT excited-state geometries.

Closer examination of molecular orbitals of CCC^{Me}-NHC-Pt^{II}-Cl (**3**) revealed a decrease in the HOMO−LUMO gap when the Cl atom was distorted out of the molecular plane. A Walsh-like diagram of the ground-state orbital energies versus constrained C_{aryl}−Pt−Cl angle at the TD-DFT S_1 excited-state geometries is included in Figure 7. This diagram demonstrates that the HOMO is more destabilized than the LUMO is stabilized as the geometry changes from the planar C_{2v} structure to the bent C_s structure.[49]

The energies in the Walsh-like diagram demonstrate the large red shift in the emission spectrum; the geometric distortion contributed to this red shift. In the C_s structure, there is a drastic change in the HOMO shape, as ligand π character is removed when the C_{aryl}−Pt−Cl angle is bent away from 180°. The p orbital of the chlorine, which has lone pair character (slightly antibonding) in the planar structure, becomes strongly Pt−Cl antibonding (σ^*) in the C_s bent structure. In the LUMO, as the C_{aryl}−Pt−Cl angle is bent away from 180°, the bent chlorine retains much of the p lone pair character but creates a small "divot" in the Pt−Cl π character. In the bent structure, both the HOMO and the LUMO have a large amount of nonbonding metal d orbital character. This unique geometric change during the electronic transition may contribute to the air stability and photostability of the complex.

■ CONCLUSION

The synthesis and characterization of the two novel CCC-NHC pincer Pt(II) complexes **1** and **2** have been reported. They display distorted-square-planar configurations, as expected for d^8 four-coordinated transition-metal compounds. Complexes **1** and **2** were found to emit bright blue light in the solid state under UV irradiation with emissions that are stable under an ambient atmosphere (O_2 and H_2O) for extended periods. At the same time, they were found to be thermally stable under an N_2 atmosphere upon evaporation, which suggests that they would be suitable for thermodeposition processing. Computational studies of the complexes illustrated the details of the molecular orbitals and the electronic transitions involved in the photophysical processes. Somewhat surprisingly, the computed gas-phase geometry of the excited state of model **3** displays a significant amount of geometric distortion, mostly about the C_{aryl}−Pt−Cl angle.

■ EXPERIMENTAL SECTION

General Procedures. All starting materials were purchased from Sigma-Aldrich, Fisher Scientific, or Strem. The reagents were used as received unless otherwise mentioned. All solvents were dried and were degassed by passing through a basic alumina column under Ar protection.[50] All reactions involving organometallic reagents were carried out under a N_2 or Ar atmosphere using standard glovebox and Schlenk line techniques. NMR spectra were collected using a Bruker Avance 300 or 500 spectrometer and were referenced to the residual solvent peak (δ in ppm, J in Hz). Electrospray ionization mass spectra were collected using a Waters Micromass ZQ mass spectrometer. Elemental analyses were carried out by Columbia Analytical Service or on a PerkinElmer 2400 Series II CHNS/O analyzer. UV−visible absorption spectra were collected using a HP 8453 UV−visible system. Emission spectra were collected using a PerkinElmer LS 55 fluorescence spectrometer. Photostability studies were carried out by exposing the solid sample to 355 nm radiation. The light source was a xenon lamp, and the detector was a photodiode array placed behind a filter next to the sample chamber. Lifetime measurements were carried out using 10 Hz pulsed 355 nm Nd:YAG laser output as the pumping source and a photomultiplier tube as the detector. TGA/DSC data were collected on PerkinElmer Pyris 1 TGA/DSC 4000, with nitrogen flow at 20 mL/min and temperature gradient set at 20 °C/min.

2-(1,3-Bis(*N*-butylimidazol-2-ylidene)phenylene)(chloro)-platinum(II) (1). 1,3-Bis(1-butylimidazolium-3-yl)benzene dichloride (0.20 g, 0.50 mmol), tetrakis(dimethylamino)zirconium (0.17 g, 0.63 mmol), and CH_2Cl_2 (~4.0 mL) were combined. The mixture was stirred for 1 h at room temperature to afford a red solution. [Pt(COD)Cl_2] (0.19 g, 0.50 mmol) was added, and the mixture was stirred vigorously at room temperature for 6 h. The reaction mixture was transferred to a round-bottom flask that contained 1 mL of distilled water, and the precipitate was removed by filtration. The filtrate was concentrated under vacuum to afford a yellow solid. The solid was washed with water (2 × 1 mL), cold CH_2Cl_2 (2 × 1 mL), and Et_2O (3 × 3 mL) and was dried under vacuum, yielding a yellow crystalline solid (0.13 g, 50%). X-ray-quality crystals were grown by slow diffusion of diethyl ether vapor into a CH_2Cl_2 solution of **1**. ^{1}H NMR (CD_2Cl_2; 300.132 MHz): δ 7.40 (dd, 2H, J = 2.0 Hz, J = 9.0 Hz, imid), 7.01 (dd, 2H, J = 2.0 Hz, J = 9.0 Hz, imid), 7.16 (t, 1H, J = 7.8 Hz, p-Ph), 6.93 (dd, 2H, J = 8.0 Hz, $^4J_{Pt-H}$ = 16.1 Hz, m-Ph), 4.69 (t, 4H, J = 7.3 Hz, NCH_2), 1.86 (quintet, 4H, J = 7.5 Hz), 1.45 (sextet, 4H, J = 7.7 Hz), 0.97 (t, 6H, J = 7.4 Hz). ^{13}C NMR (d_6-DMSO; 75.476 MHz, 350 K): δ 171.7 ($^1J_{Pt-C}$ = 1168 Hz), 144.1, 133.8 ($^1J_{Pt-C}$ = 937 Hz), 123.3, 121.1, 115.7, 107.6, 47.7, 32.7, 18.8, 13.2. ESI-MS: calcd for $C_{20}H_{25}ClN_4PtNa$ [M + Na] (m/z) 575 (100%), 574 (93%), 573 (74%), 576 (45%), 577 (42%); found 575 (100%), 574 (96%), 573 (78%), 576 (46%), 577 (43%). Anal. Calcd: C, 43.52; H, 4.57; N, 10.15. Found: C, 43.19; H, 4.09; N, 9.90.

2-(1,3-Bis(*N*-butylimidazol-2-ylidene)phenylene)(bromo)-platinum(II) (2). 1,3-Bis(1-butylimidazolium-3-yl)benzene dibromide (0.48 g, 1.0 mmol), tetrakis(dimethylamino)zirconium (0.32 g, 1.2 mmol), and THF (10 mL) were stirred for 1 h at room temperature, yielding a cloudy suspension. [Pt(COD)Br_2] (0.463 g, 1.0 mmol) was added, and the reaction mixture was stirred at room temperature for 8 h, yielding a cloudy yellow suspension. After standing for 10 min, a yellow precipitate was observed with a clear reddish supernatant liquid. The precipitate was collected and washed with toluene (3 × 3 mL), yielding an analytically pure yellow solid (0.242 g, 52%). Some of the solid was directly used for X-ray crystallography. ^{1}H NMR (CD_2Cl_2; 300.132 MHz): δ 7.40 (dd, 2H, J = 2.0 Hz, J = 9.0 Hz, imid), 7.01 (dd, 2H, J = 2.0 Hz, J = 9.0 Hz, imid), 7.18 (t, 1H, J = 7.8 Hz, p-Ph), 6.93 (dd, 2H, J = 8.0 Hz, $^4J_{Pt-H}$ = 17.8 Hz, m-Ph), 4.76 (t, 4H, J = 7.3 Hz, NCH_2), 1.87 (quintet, 4H, J = 7.5 Hz), 1.45 (sextet, 4H, J = 7.7 Hz), 0.97 (t, 6H, J = 7.4 Hz). ^{13}C NMR (d_6-DMSO; 75.476 MHz, 350 K): δ 170.5 ($^1J_{Pt-C}$ = 1166 Hz), 143.8, 134.0 ($^1J_{Pt-C}$ = 953 Hz), 122.8, 121.3, 115.4, 107.5, 48.3, 32.8, 18.6, 13.1. ESI-MS: calcd for $C_{20}H_{25}BrN_4Pt$ [M^+] (m/z) 595.1; found 595.0. Anal. Calcd: C, 40.28; H, 4.22; N, 9.39. Found: C, 40.10; H, 3.94; N, 9.30.

X-ray Crystallography. X-ray-quality crystals of **1** and **2** were mounted atop fine glass fibers. Diffraction experiments were performed on an Oxford Diffraction Systems Gemini S diffractometer with Mo Kα radiation (λ = 0.710 73 Å) at 298 K. The structures were solved and refined using the SHELX suite of programs.

Computational Details. Most of the presented theoretical calculations were carried out using the Gaussian09[51] implementation of B3LYP (the B3 exchange functional[52] and LYP correlation functional)[53] density functional theory (DFT),[54] using the default pruned fine grids for energies (75, 302), default pruned coarse grids for gradients and Hessians (35, 110) (neither grid was pruned for platinum), and nondefault SCF convergence for geometry optimizations (10^{-6}). Excited states were geometry optimized using analytical gradients[55] with time-dependent density functional theory (TD-DFT)[56] calculations. TD-DFT geometry optimizations were performed for the first three excited singlet states. In most cases, 20 singlet excitations were solved iteratively (TD(ROOT=X, NSTATES=20), where X was the root number). However, in cases where during the optimization the Davidson iterative solution of the excitations failed to converge, 40 singlet excitations were solved iteratively. Symmetry was disabled during all excited-state geometry optimizations; however, the S_1 geometry was optimized to have C_s symmetry. For TD-DFT optimizations, the default convergence criteria for the energy (10^{-6}) and nondefault convergence criteria for the wave function (10^{-6}) were used. The C_{aryl}−Pt−Cl angle was constrained (from the S_1 optimized angle of 93.31° to 180°) in a series of TD-DFT optimizations for the first root. A Walsh-like diagram was constructed from the ground-state orbital energies at the TD-DFT excited-state geometries. All calculations were conducted with the same basis set combination. The basis set for platinum was the Hay and Wadt basis set and effective core potential (ECP) combination (LanL2DZ)[57] as modified by Couty and Hall, where the two outermost p functions have been replaced by a (41) split of the optimized platinum 6p functions.[58] The 6-31G(d′) basis sets[59] were used for all other atoms. Spherical harmonic d functions were used throughout; i.e., there are five angular basis functions per d function. In all computations, the *n*-butyl group of the ligand was trimmed to methyl. All structures were fully optimized, and frequency calculations (analytical for DFT and numerical for TD-DFT) were performed on all ground and select excited-state structures to ensure that either a zeroth-order saddle point (a local minimum) or a first-order saddle point was achieved. To analyze the electronic structure of the TD-DFT excited states on roots with high oscillator strength, a natural transition orbital (NTO) analysis[60] was performed. The NTO analysis diagonalized the transition density matrix and gave a representation of the electronic excitation in terms of a single excited particle and empty hole. While the ordering of the natural transition orbitals was slightly different from that of the ground state molecular orbitals, the NTOs and MOs appeared to be qualitatively similar. All molecular orbital plots represented in the article are ground-state Kohn−Sham orbitals at either the ground-state or excited-state geometries. The computed absorption spectrum was calculated from the vertical transitions obtained from TD-DFT single-point calculations on the optimized ground-state geometry. The geometry optimization from the vertical excitation from the ground state produced a transition state (verified by a numerical frequency calculation) that perturbed the C_{aryl}−Pt−Cl angle away from 180°. The computed emission spectrum was calculated using the fully optimized, minimum-energy geometry of the S_1 excited state. The computationally derived absorption and emission spectra were simulated with an in-house Fortran program by convoluting[61] the computed excitation energies and computed oscillator strengths with a Gaussian line shape and a broadening of 20 nm.

In order to investigate the possibility that the observed emission spectrum comes from the planar triplet excited state, we computed spectra including spin−orbit coupling. PBE (the PBE exchange correction and correlation correction[62]) density functional theory[54] computations were performed with the Amsterdam Density Functional program (ADF, version 2008.01).[63] ADF uses Slater-type orbital (STO) basis sets rather than Gaussian-type orbitals (GTO) and contains a density fitting procedure using auxiliary functions (fit functions) for the evaluation of the Coulomb potential and molecular density. All reported ADF calculations used gradient corrections to the LDA (local density approximation) density functional energy during the SCF, utilized a single-point grid accuracy factor (4.0), and used the default SCF convergence (10^{-8}). Relativistic effects were treated with the zeroth-order regular approximation (ZORA)[64] with the default sum of atoms potential approximation (SAPA) potential.[65] The frozen core approximation was used. The basis set used in ADF calculations utilized the standard ADF ZORA TZ2P basis sets for all atoms (an uncontracted triple-ζ STO basis set with two polarization functions). ADF ZORA basis sets have been optimized for use within ZORA relativistic calculations. Excitation energies were computed with time-dependent density functional theory (TD-DFT)[66] with a Hamiltonian that includes spin−orbit coupling (i.e., spin−orbit coupling is included self-consistently in the wave function).[67] All geometries used in ADF calculations were from Gaussian 09 optimizations. A description of these results is included in the Supporting Information. Molecular orbitals in Figure 5 were visualized with JIMP 2.[68]

■ ASSOCIATED CONTENT

Ⓢ Supporting Information

Figures, tables, text, and CIF files giving TGA, DSC spectra, and detailed crystallographic data for CCC^{Bu}-NHC-Pt^{II}-X complexes **1** and **2**, as well as Cartesian coordinates for optimized geometries and detailed computed TD-DFT emission/absorption spectra for CCC^{Me}-NHC-Pt^{II}-Cl (**3**). This material is available free of charge via the Internet at http://pubs.acs.org.

■ AUTHOR INFORMATION

Corresponding Author

*Fax: (662)915-7300. Tel: (662)915-5337. E-mail: hollis@olemiss.edu (T.K.H.); nhammer@olemiss.edu (N.I.H.); cewebstr@memphis.edu (C.E.W.).

■ ACKNOWLEDGMENTS

We gratefully acknowledge the National Science Foundation (NSF Grant Nos. CHE0911528, CHE0809732, CHE955550, EPS0903787, MRI0421319, and MRI0618148), The University of Mississippi, and The University of Memphis for financial support and The University of Memphis High Performance Computing Facility and Computational Research on Materials Institute at the University of Memphis (CROMIUM) for computing support. We thank Professor John M. Rimoldi, Sarah Chajkowski, and Rob Smith for assistance with collecting mass spectral data and elemental analyses, Professor Randy Wadkins for assistance with quantum efficiency measurements, Professor Jason Ritchie for assistance with DSC measurements, and Professor Soumyajit Majumdar and Sindhuri Maddineni for assistance with TGA measurements.

■ REFERENCES

(1) (a) Igau, A.; Grutzmacher, H.; Baceiredo, A.; Bertrand, G. *J. Am. Chem. Soc.* **1988**, *110*, 6463−6466. (b) Arduengo, A. J. III; Harlow, R. L.; Kline, M. *J. Am. Chem. Soc.* **1991**, *113*, 361−363. (c) Bourissou, D.; Guerret, O.; Gabbai, F. P.; Bertrand, G. *Chem. Rev.* **2000**, *100*, 39−91. (d) de Frémont, P.; Marion, N.; Nolan, S. P. *Coord. Chem. Rev.* **2009**, *253*, 862−892.

(2) (a) Arduengo, A. J.; Dias, H. V. R.; Harlow, R. L.; Kline, M. *J. Am. Chem. Soc.* **1992**, *114*, 5530−5534. (b) Arduengo, A. J.; Goerlich, J. R.; Marshall, W. J. *J. Am. Chem. Soc.* **1995**, *117*, 11027−11028.

(3) Alder, R. W.; Allen, P. R.; Murray, M.; Orpen, A. G. *Angew. Chem., Int. Ed. Engl.* **1996**, *35*, 1121−1123.

(4) (a) Crudden, C. M.; Allen, D. P. *Coord. Chem. Rev.* **2004**, *248*, 2247−2273. (b) Cavallo, L.; Correa, A.; Costabile, C.; Jacobsen, H. *J. Organomet. Chem.* **2005**, *690*, 5407−5413. (c) Scott, N. M.; Nolan, S. P. *Eur. J. Inorg. Chem.* **2005**, 1815−1828. (d) Lee, H. M.; Lee, C. C.; Cheng, P. Y. *Curr. Org. Chem.* **2007**, *11*, 1491−1524. (e) Schuster, O.; Yang, L.; Raubenheimer, H. G.; Albrecht, M. *Chem. Rev.* **2009**, *109*, 3445−3478. (f) Hahn, F. E.; Jahnke, M. C. *Angew. Chem., Int. Ed.* **2008**, *47*, 3122−3172. (g) Gil, W.; Trzeciak, A. M. *Coord. Chem. Rev.* **2011**, *255*, 473−483. (h) Jacobsen, H.; Correa, A.; Poater, A.; Costabile, C.; Cavallo, L. *Coord. Chem. Rev.* **2009**, *253*, 687−703.

(5) (a) McReynolds, M. D.; Dougherty, J. M.; Hanson, P. R. *Chem. Rev.* **2004**, *104*, 2239−2258. (b) Grubbs, R. H.; Miller, S. J.; Fu, G. C. *Acc. Chem. Res.* **1995**, *28*, 446−452. (c) Monfette, S.; Fogg, D. E. *Chem. Rev.* **2009**, *109*, 3783−3816. (d) Tallarico, J. A.; Randall, M. L.; Snapper, M. L. *Tetrahedron* **1997**, *53*, 16511−16520. (e) Buchmeiser, M. R. *Chem. Rev.* **2000**, *100*, 1565−1604. (f) Chatterjee, A. K.; Choi, T.-L.; Sanders, D. P.; Grubbs, R. H. *J. Am. Chem. Soc.* **2003**, *125*, 11360−11370. (g) Connon, S. J.; Blechert, S. *Angew. Chem., Int. Ed.* **2003**, *42*, 1900−1923. (h) Lozano-Vila, A. M.; Monsaert, S.; Bajek, A.; Verpoort, F. *Chem. Rev.* **2010**, *110*, 4865−4909.

(6) Herrmann, W. A.; Elison, M.; Fischer, J.; Kocher, C.; Artus, G. R. J. *Angew. Chem., Int. Ed. Engl.* **1995**, *34*, 2371−2374.

(7) (a) Altenhoff, G.; Goddard, R.; Lehmann, C. W.; Glorius, F. *J. Am. Chem. Soc.* **2004**, *126*, 15195−15201. (b) Huynh, H. V.; Han, Y.; Ho, J. H. H.; Tan, G. K. *Organometallics* **2006**, *25*, 3267−3274. (c) Marion, N.; Navarro, O.; Mei, J.; Stevens, E. D.; Scott, N. M.; Nolan, S. P. *J. Am. Chem. Soc.* **2006**, *128*, 4101−4111.

(8) Valente, C.; Belowich, M. E.; Hadei, N.; Organ, M. G. *Eur. J. Org. Chem.* **2010**, *2010*, 4343−4354.

(9) McGuinness, D. S.; Cavell, K. J. *Organometallics* **2000**, *19*, 741−748.

(10) Broggi, J.; Clavier, H.; Nolan, S. P. *Organometallics* **2008**, *27*, 5525−5531.

(11) (a) Hillier, A. C.; Grasa, G. A.; Viciu, M. S.; Lee, H. M.; Yang, C. L.; Nolan, S. P. *J. Organomet. Chem.* **2002**, *653*, 69−82. (b) Samojłowicz, C.; Bieniek, M.; Grela, K. *Chem. Rev.* **2009**, *109*, 3708−3742. (c) Díez-González, S.; Marion, N.; Nolan, S. P. *Chem. Rev.* **2009**, *109*, 3612−3676. (d) Nair, V.; Vellalath, S.; Babu, B. P. *Chem. Soc. Rev.* **2008**, *37*, 2691−2698.

(12) (a) Marion, N.; Ecarnot, E. C.; Navarro, O.; Amoroso, D.; Bell, A.; Nolan, S. P. *J. Org. Chem.* **2006**, *71*, 3816−3821. (b) Demir, S.; Özdemir, I.; Çetinkaya, B.; Arslan, H.; VanDerveer, D. *Polyhedron* **2011**, *30*, 195−200.

(13) (a) Fujihara, T.; Obora, Y.; Tokunaga, M.; Sato, H.; Tsuji, Y. *Chem. Commun.* **2005**, 4526−4528. (b) Ohta, H.; Fujihara, T.; Tsuji, Y. *Dalton Trans.* **2008**, 379−385.

(14) Beletskaya, I. P.; Kashin, A. N.; Litvinov, A. E.; Tyurin, V. S.; Valetsky, P. M.; van Koten, G. *Organometallics* **2006**, *25*, 154−158.

(15) (a) Au, V. K. M.; Wong, K. M. C.; Zhu, N. Y.; Yam, V. W. W. *J. Am. Chem. Soc.* **2009**, *131*, 9076−9085. (b) Sajoto, T.; Djurovich, P. I.; Tamayo, A.; Yousufuddin, M.; Bau, R.; Thompson, M. E.; Holmes, R. J.; Forrest, S. R. *Inorg. Chem.* **2005**, *44*, 7992−8003. (c) Unger, Y.; Zeller, A.; Ahrens, S.; Strassner, T. *Chem. Commun.* **2008**, 3263−3265. (d) Wu, Y.; Wu, S. X.; Li, H. B.; Geng, Y.; Su, Z. M. *Dalton Trans.* **2011**, *40*, 4480−4488. (e) Mizuhata, Y.; Sasamori, T.; Tokitoh, N. *Chem. Rev.* **2009**, *109*, 3479−3511. (f) Hindi, K. M.; Panzner, M. J.; Tessier, C. A.; Cannon, C. L.; Youngs, W. J. *Chem. Rev.* **2009**, *109*, 3859−3884. (g) Arnold, P. L.; Casely, I. J. *Chem. Rev.* **2009**, *109*, 3599−3611. (h) Chi, Y.; Chou, P. T. *Chem. Soc. Rev.* **2010**, *39*, 638−655.

(16) (a) Stetter, H.; Rämsch, R. Y.; Kuhlmann, H. *Synthesis* **1976**, *11*, 733−735. (b) Henrique Teles, J.; Melder, J.-P.; Ebel, K.; Schneider, R.; Gehrer, E.; Harder, W.; Brode, S.; Enders, D.; Breuer, K.; Raabe, G. *Helv. Chim. Acta* **1996**, *79*, 61−83. (c) Matsumoto, T.; Yamamoto, H.; Inoue, S. *J. Am. Chem. Soc.* **1984**, *106*, 4829−4832. (d) Matsumoto, T.; Inoue, S. *J. Chem. Soc., Chem. Commun.* **1983**, 171−172.

(17) (a) Stetter, H. *Angew. Chem., Int. Ed. Engl.* **1976**, *15*, 639−647. (b) Kerr, M. S.; Read de Alaniz, J.; Rovis, T. *J. Am. Chem. Soc.* **2002**, *124*, 10298−10299.

(18) (a) Enders, D.; Niemeier, O.; Henseler, A. *Chem. Rev.* **2007**, *107*, 5606−5655. (b) Powell, A. B.; Suzuki, Y.; Ueda, M.; Bielawski, C. W.; Cowley, A. H. *J. Am. Chem. Soc.* **2011**, *133*, 5218−5220. (c) Cesar, V.; Bellemin-Laponnaz, S.; Gade, L. H. *Chem. Soc. Rev.* **2004**, *33*, 619−636.

(19) (a) Crocker, C.; Errington, R. J.; McDonald, W. S.; Odell, K. J.; Shaw, B. L.; Goodfellow, R. J. *J. Chem. Soc., Chem. Commun.* **1979**, 498−499. (b) Morales-Morales, D.; Jensen, C. M.; *The Chemistry of Pincer Compounds*; Elsevier: New York, 2007. (c) Jones, N. D.; Cavell, R. G. *J. Organomet. Chem.* **2005**, *690*, 5485−5496. (d) Gagliardo, M.; Snelders, D. J. M.; Chase, P. A.; Klein Gebbink, R. J. M.; van Klink, G. P. M; van Koten, G. *Angew. Chem., Int. Ed.* **2007**, *46*, 8558−8573. (e) van der Boom, M. E.; Milstein, D. *Chem. Rev.* **2003**, *103*, 1759−1792.

(20) (a) Chen, J. C. C.; Lin, I. J. B. *Dalton Trans.* **2000**, 839−840. (b) Tulloch, A. A. D.; Danopoulos, A. A.; Tizzard, G. J.; Coles, S. J.; Hursthouse, M. B.; Hay-Motherwell, R. S.; Motherwell, W. B. *Chem. Commun.* **2001**, 1270−1271. (c) Peris, E.; Loch, J. A.; Mata, J.; Crabtree, R. H. *Chem. Commun.* **2001**, 201−202. (d) Peris, E.; Crabtree, R. H. *Coord. Chem. Rev.* **2004**, *248*, 2239−2246. (e) Peris, E.; Crabtree Robert, H. In *The Chemistry of Pincer Compounds*; Morales-Morales, D., Jensen, C. M., Eds.; Elsevier: New York, 2007, pp 107−124. (f) Poyatos, M.; Mata, J. A.; Peris, E. *Chem. Rev.* **2009**, *109*, 3677−3707. (g) Pugh, D.; Danopoulos, A. A. *Coord. Chem. Rev.* **2007**, *251*, 610−641. (h) Corberan, R.; Mas-Marza, E.; Peris, E. *Eur. J. Inorg. Chem.* **2009**, 1700−1716. (i) Melaimi, M.; Soleilhavoup, M.; Bertrand, G. *Angew. Chem., Int. Ed.* **2010**, *49*, 8810−8849.

(21) (a) Hahn, F. E.; Jahnke, M. C.; Pape, T. *Organometallics* **2007**, *26*, 150−154. (b) Danopoulos, A. A.; Tulloch, A. A. D.; Winston, S.; Eastham, G.; Hursthouse, M. B. *Dalton Trans.* **2003**, 1009−1015. (c) Grundemann, S.; Albrecht, M.; Loch, J. A.; Faller, J. W.; Crabtree, R. H. *Organometallics* **2001**, *20*, 5485−5488. (d) Schultz, K. M.; Goldberg, K. I.; Gusev, D. G.; Heinekey, D. M. *Organometallics* **2011**, *30*, 1429−1437. (e) Lv, K.; Cui, D. *Organometallics* **2010**, *29*, 2987−2993.

(22) (a) Hahn, F. E.; Jahnke, M. C.; Gomez-Benitez, V.; Morales-Morales, D.; Pape, T. *Organometallics* **2005**, *24*, 6458−6463. (b) Nielsen, D. J.; Cavell, K. J.; Skelton, B. W.; White, A. H. *Inorg. Chim. Acta* **2002**, *327*, 116−125.

(23) (a) Cho, J.; Hollis, T. K.; Helgert, T. R.; Valente, E. J. *Chem. Commun.* **2008**, 5001−5003. (b) Bauer, E. B.; Andavan, G. T. S.; Hollis, T. K.; Rubio, R. J.; Cho, J.; Kuchenbeiser, G. R.; Helgert, T. R.; Letko, C. S.; Tham, F. S. *Org. Lett.* **2008**, *10*, 1175−1178. (c) Rubio, R. J.; Andavan, G. T. S.; Bauer, E. B.; Hollis, T. K.; Cho, J.; Tham, F. S.; Donnadieu, B. *J. Organomet. Chem.* **2005**, *690*, 5353−5364. (d) Cho, J.; Hollis, T. K.; Valente, E. J.; Trate, J. M. *J. Organomet. Chem.* **2011**, *696*, 373−377.

(24) (a) Pugh, D.; Boyle, A.; Danopoulos, A. A. *Dalton Trans.* **2008**, 1087−1094. (b) Danopoulos, A. A.; Pugh, D.; Wright, J. A. *Angew. Chem., Int. Ed.* **2008**, *47*, 9765−9767. (c) Loch, J. A.; Albrecht, M.; Peris, E.; Mata, J.; Faller, J. W.; Crabtree, R. H. *Organometallics* **2002**, *21*, 700−706. (d) Poyatos, M.; Mata, J. A.; Falomir, E.; Crabtree, R. H.; Peris, E. *Organometallics* **2003**, *22*, 1110−1114. (e) Danopoulos, A. A.; Tsoureas, N.; Wright, J. A.; Light, M. E. *Organometallics* **2003**, *23*, 166−168. (f) McGuinness, D. S.; Gibson, V. C.; Steed, J. W. *Organometallics* **2004**, *23*, 6288−6292. (g) Danopoulos, A. A.; Wright, J. A.; Motherwell, W. B.; Ellwood, S. *Organometallics* **2004**, *23*, 4807−4810. (h) Serra, D.; Cao, P.; Cabrera, J.; Padilla, R.; Rominger, F.; Limbach, M. *Organometallics* **2011**, *30*, 1885−1895.

(25) (a) Chianese, A. R.; Mo, A.; Lampland, N. L.; Swartz, R. L.; Bremer, P. T. *Organometallics* **2010**, *29*, 3019−3026. (b) Raynal, M.; Pattacini, R.; Cazin, C. S. J.; Vallee, C.; Olivier-Bourbigou, H.; Braunstein, P. *Organometallics* **2009**, *28*, 4028−4047.

(26) (a) Moore, T. A.; Gust, D.; Mathis, P.; Mialocq, J. C.; Chachaty, C.; Bensasson, R. V.; Land, E. J.; Doizi, D.; Liddell, P. A.; Lehman, W. R.; Nemeth, G. A.; Moore, A. L. *Nature* **1984**, *307*, 630−632. (b) Gust, D.; Moore, T. A.; Moore, A. L. *Acc. Chem. Res.* **2001**, *34*, 40−48. (c) Chakraborty, S.; Wadas, T. J.; Hester, H.; Schmehl, R.; Eisenberg, R. *Inorg. Chem.* **2005**, *44*, 6865−6878. (d) Wasielewski, M. R. *Chem. Rev.* **1992**, *92*, 435−461. (e) Hambourger, M.; Moore, G. F.; Kramer, D. M.; Gust, D.; Moore, A. L.; Moore, T. A. *Chem. Soc. Rev.* **2009**, *38*, 25−35.

(27) (a) Archer, M. D.; Bolton, J. R. *J. Phys. Chem.* **1990**, *94*, 8028−8036. (b) Borja, M.; Dutta, P. K. *Nature* **1993**, *362*, 43−45. (c) Bard, A. J.; Fox, M. A. *Acc. Chem. Res.* **1995**, *28*, 141−145. (d) Jarosz, P.; Du, P. W.; Schneider, J.; Lee, S. H.; McCamant, D.; Eisenberg, R. *Inorg. Chem.* **2009**, *48*, 9653−9663. (e) Navarro, R. M.; Alvarez-Galvan, M. C.; de la Mano, J. A. V.; Al-Zahrani, S. M.; Fierro, J. L. G. *Energy Environ. Sci.* **2010**, *3*, 1865−1882. (f) Walter, M. G.; Warren, E. L.; McKone, J. R.; Boettcher, S. W.; Mi, Q. X.; Santori, E. A.; Lewis, N. S. *Chem. Rev.* **2010**, *110*, 6446−6473.

(28) (a) Becquerel, A.-E. *C. R. Acad. Sci. Paris* **1839**, *9*, 561. (b) Mayo, E. I.; Kilsa, K.; Tirrell, T.; Djurovich, P. I.; Tamayo, A.; Thompson, M. E.; Lewis, N. S.; Gray, H. B. *Photochem. Photobiol. Sci.* **2006**, *5*, 871−873. (c) Helgesen, M.; Sondergaard, R.; Krebs, F. C. *J. Mater. Chem.* **2010**, *20*, 36−60.

(29) (a) Tang, C. W.; Vanslyke, S. A. *Appl. Phys. Lett.* **1987**, *51*, 913−915. (b) Burroughes, J. H.; Bradley, D. D. C.; Brown, A. R.; Marks, R. N.; Mackay, K.; Friend, R. H.; Burns, P. L.; Holmes, A. B. *Nature* **1990**, *347*, 539−541. (c) Bauer, R.; Finkenzeller, W. J.; Bogner, U.; Thompson, M. E.; Yersin, H. *Org. Electron.* **2008**, *9*, 641−648. (d) Finkenzeller, W. J.; Hofbeck, T.; Thompson, M. E.; Yersin, H. *Inorg. Chem.* **2007**, *46*, 5076−5083. (e) Finkenzeller, W. J.; Thompson, M. E.; Yersin, H. *Chem. Phys. Lett.* **2007**, *444*, 273−279. (f) Zhong, C. M.; Duan, C. H.; Huang, F.; Wu, H. B.; Cao, Y. *Chem. Mater.* **2011**, *23*, 326−340.

(30) (a) Moudam, O.; Rowan, B. C.; Alamiry, M.; Richardson, P.; Richards, B. S.; Jones, A. C.; Robertson, N. *Chem. Commun.* **2009**, 6649−6651. (b) Tam, A. Y.-Y.; Wong, K. M.-C.; Yam, V. W.-W. *J. Am. Chem. Soc.* **2009**, *131*, 6253−6260.

(31) Lee, C. S.; Sabiah, S.; Wang, J. C.; Hwang, W. S.; Lin, I. J. B. *Organometallics* **2010**, *29*, 286−289.

(32) Vargas, V. C.; Rubio, R. J.; Hollis, T. K.; Salcido, M. E. *Org. Lett.* **2003**, *5*, 4847−4849.

(33) Spencer, L. P.; Winston, S.; Fryzuk, M. D. *Organometallics* **2004**, *23*, 3372−3374.

(34) (a) Ahrens, S.; Strassner, T. *Inorg. Chim. Acta* **2006**, *359*, 4789−4796. (b) Berthon-Gelloz, G.; Buisine, O.; Briere, J. F.; Michaud, G.;

Sterin, S.; Mignani, G.; Tinant, B.; Declercq, J. P.; Chapon, D.; Marko, I. E. *J. Organomet. Chem.* **2005**, *690*, 6156−6168.

(35) Farrugia, L. *J. Appl. Crystallogr.* **1997**, *30*, 565.

(36) (a) Vanderploeg, A.; Vankoten, G.; Vrieze, K.; Spek, A. L. *Inorg. Chem.* **1982**, *21*, 2014−2026. (b) Fantasia, S.; Petersen, J. L.; Jacobsen, H.; Cavallo, L.; Nolan, S. P. *Organometallics* **2007**, *26*, 5880−5889.

(37) Yersin, H.; Donges, D. In *Transition Metal and Rare Earth Compounds*; Yersin, H., Ed.; Springer: Berlin/Heidelberg, Germany, 2001; Vol. *214*, pp 81−186.

(38) Drago, R. S. *Physical Methods in Chemistry*; Saunders: Philadelphia, PA, 1977.

(39) (a) Zhang, L. Y.; Li, B.; Shi, L. F.; Li, W. L. *Opt. Mater.* **2009**, *31*, 905−911. (b) Evans, R. C.; Douglas, P.; Winscom, C. J. *Coord. Chem. Rev.* **2006**, *250*, 2093−2126. (c) Unger, Y.; Meyer, D.; Strassner, T. *Dalton Trans.* **2010**, *39*, 4295−4301.

(40) Unger, Y.; Zeller, A.; Taige, M. A.; Strassner, T. *Dalton Trans.* **2009**, 4786−4794.

(41) (a) Walser, A. D.; Priestley, R.; Dorsinville, R. *Synth. Met.* **1999**, *102*, 1552−1553. (b) Martin, R. L.; Kress, J. D.; Campbell, I. H.; Smith, D. L. *Phys. Rev. B* **2000**, *61*, 15804. (c) Colle, M.; Garditz, C. *Appl. Phys. Lett.* **2004**, *84*, 3160−3162.

(42) Seo, J. H.; Kim, I. J.; Kim, Y. K.; Kim, Y. S. *Thin Solid Films* **2008**, *516*, 3614−3617.

(43) (a) Du, Y.; Fu, Y.; Shi, Y.; Lü, X.; Lü, C.; Su, Z. *J. Solid State Chem.* **2009**, *182*, 1430−1437. (b) Kai, Y.; Morita, M.; Yasuoka, N.; Kasai, N. *Bull. Chem. Soc. Jpn.* **1985**, *58*, 1631−1635.

(44) (a) Tao, X. T.; Suzuki, H.; Wada, T.; Miyata, S.; Sasabe, H. *J. Am. Chem. Soc.* **1999**, *121*, 9447−9448. (b) Tao, X. T.; Suzuki, H.; Wada, T.; Sasabe, H.; Miyata, S. *Appl. Phys. Lett.* **1999**, *75*, 1655−1657. (c) Vinyard, D. J.; Richter, M. M. *Dalton Trans.* **2006**, 4461−4464.

(45) Shi, L. L.; Li, T.; Zhao, S. S.; Li, H.; Su, Z. M. *Theor. Chem. Acc.* **2009**, *124*, 29−36.

(46) Halls, M. D.; Schlegel, H. B. *Chem. Mater.* **2001**, *13*, 2632−2640.

(47) Jakubikova, E.; Chen, W.; Dattelbaum, D. M.; Rein, F. N.; Rocha, R. C.; Martin, R. L.; Batista, E. R. *Inorg. Chem.* **2009**, *48*, 10720−10725.

(48) The bent T$_1$ (triplet-ES C_s) species and the planar T$_1$ (triplet-ES C_{2v}) species are very close in energy (0.8 kcal mol^{-1}) but dissimilar in geometry. The bent S$_1$ (singlet-ES C_s) species and bent T$_1$ species are quite similar in geometry (rmsd = 0.134 Å for all atoms and 0.0457 Å for all atoms other than chlorine) but are separated by 9.5 kcal mol^{-1}. The TD-DFT PBE-ZORA-SO computed spectra (see the Supporting Information for further computational details) for both the bent S$_1$ and bent T$_1$ match reasonably with the experimental observations in Figure 2a (see Figures S12 and S13 in the Supporting Information) and are in qualitative agreement with the B3LYP computed spectra included in Figures 4 and 6.

(49) We speculate that there is orbital crossing occurring of the excited state orbitals, but we cannot prove that with the results from TD-DFT calculations.

(50) Pangborn, A. B.; Giardello, M. A.; Grubbs, R. H.; Rosen, R. K.; Timmers, F. J. *Organometallics* **1996**, *15*, 1518−1520.

(51) Frisch, M. J. et al. *Gaussian 09, Revision A.02*; Gaussian, Inc., Wallingford, CT, 2009.

(52) Becke, A. D. *J. Chem. Phys.* **1993**, *98*, 5648−5652.

(53) Lee, C.; Yang, W.; Parr, R. G. *Phys. Rev. B* **1988**, *37*, 785.

(54) Parr, R. G.; Yang, W. *Density Functional Theory of Atoms and Molecules*; Oxford University Press: New York, 1989.

(55) (a) Furche, F.; Ahlrichs, R. *J. Chem. Phys.* **2002**, *117*, 7433−7447. (b) Furche, F.; Ahlrichs, R. *J. Chem. Phys.* **2004**, *121*, 12772−12773.

(56) Marques, M. A. L.; Gross, E. K. U. *Annu. Rev. Phys. Chem.* **2004**, *55*, 427−455.

(57) Hay, P. J.; Wadt, W. R. *J. Chem. Phys.* **1985**, *82*, 299−310.

(58) Couty, M.; Hall, M. B. *J. Comput. Chem.* **1996**, *17*, 1359−1370.

(59) (a) Hehre, W. J.; Ditchfie., R; Pople, J. A. *J. Chem. Phys.* **1972**, *56*, 2257−2261. (b) Hariharan, P. C.; Pople, J. A. *Theor. Chim. Acta* **1973**, *28*, 213−222.

(60) Martin, R. L. *J. Chem. Phys.* **2003**, *118*, 4775−4777.

(61) Press, W. H. *Numerical Recipes: The Art of Scientific Computing*; Cambridge University Press: London, 1992.

(62) (a) Perdew, J. P.; Burke, K.; Ernzerhof, M. *Phys. Rev. Lett.* **1997**, *78*, 1396−1396. (b) Perdew, J. P.; Burke, K.; Ernzerhof, M. *Phys. Rev. Lett.* **1996**, *77*, 3865−3868.

(63) (a) Guerra, C. F.; Snijders, J. G.; te Velde, G.; Baerends, E. J. *Theor. Chem. Acc.* **1998**, *99*, 391−403. (b) Bickelhaupt, F. M.; Velde, G. T.; Baerends, E. J.; Guerra, C. F.; Van Gisbergen, S. J. A.; Snijders, J. G.; Ziegler, T. *J. Comput. Chem.* **2001**, *22*, 931−967. (c) Baerends, E. J.; Autschbach, J.; Bashford, D.; Bérces, A.; Bickelhaupt, F. M.; Bo, C.; Boerrigter, P. M.; Cavallo, L.; Chong, D. P.; Deng, L.; Dickson, R. M.; Ellis, D. E.; van Faassen, M.; Fan, L.; Fischer, T. H.; Fonseca Guerra, C.; Ghysels, A.; Giammona, A.; van Gisbergen, S. J. A.; Götz, A. W.; Groeneveld, J. A.; Gritsenko, O. V.; Grüning, M.; Gusarov, S.; Harris, F. E.; van den Hoek, P.; Jacob, C. R.; Jacobsen, H.; Jensen, L.; Kaminski, J. W.; van Kessel, G.; Kootstra, F.; Kovalenko, A.; Krykunov, M. V.; van Lenthe, E.; McCormack, D. A.; Michalak, A.; Mitoraj, M.; Neugebauer, J.; Nicu, V. P.; Noodleman, L.; Osinga, V. P.; Patchkovskii, S.; Philipsen, P. H. T.; Post, D.; Pye, C. C.; Ravenek, W.; Rodríguez, J. I.; Ros, P.; Schipper, P. R. T.; Schreckenbach, G.; Seldenthuis, J. S.; Seth, M.; Snijders, J. G.; Solà, M.; Swart, M.; Swerhone, D.; te Velde, G.; Vernooijs, P.; Versluis, L.; Visscher, L.; Visser, O.; Wang, F.; Wesolowski, T. A.; van Wezenbeek, E. M.; Wiesenekker, G.; Wolff, S. K.; Woo, T. K.; Yakovlev, A. L. *ADF2008.01*; SCM, Theoretical Chemistry, Vrije Universiteit, Amsterdam, The Netherlands.

(64) (a) Chang, C.; Pelissier, M.; Durand, P. *Phys. Scr.* **1986**, *34*, 394−404. (b) van Lenthe, E.; Baerends, E. J.; Snijders, J. G. *J. Chem. Phys.* **1993**, *99*, 4597−4610. (c) van Lenthe, E.; Baerends, E. J.; Snijders, J. G. *J. Chem. Phys.* **1994**, *101*, 9783−9792. (d) van Lenthe, E.; van Leeuwen, R.; Baerends, E. J.; Snijders, J. G. *Int. J. Quantum Chem.* **1996**, *57*, 281−293. (e) van Lenthe, E.; Ehlers, A.; Baerends, E. J. *J. Chem. Phys.* **1999**, *110*, 8943−8953. (f) van Lenthe, E.; Snijders, J. G.; Baerends, E. J. *J. Chem. Phys.* **1996**, *105*, 6505−6516.

(65) Philipsen, P. H. T.; van Lenthe, E.; Snijders, J. G.; Baerends, E. J. *Phys. Rev. B* **1997**, *56*, 13556−13562.

(66) (a) van Gisbergen, S. J. A.; Snijders, J. G.; Baerends, E. J. *Comput. Phys. Commun.* **1999**, *118*, 119−138. (b) van Gisbergen, S. J. A.; Kootstra, F.; Schipper, P. R. T.; Gritsenko, O. V.; Snijders, J. G.; Baerends, E. J. *Phys. Rev. A* **1998**, *57*, 2556−2571. (c) Bauernschmitt, R.; Ahlrichs, R. *Chem. Phys. Lett.* **1996**, *256*, 454−464. (d) Jamorski, C.; Casida, M. E.; Salahub, D. R. *J. Chem. Phys.* **1996**, *104*, 5134−5147. (e) van Gisbergen, S. J. A.; Groeneveld, J. A.; Rosa, A.; Snijders, J. G.; Baerends, E. J. *J. Phys. Chem. A* **1999**, *103*, 6835−6844. (f) van Gisbergen, S. J. A.; Snijders, J. G.; Baerends, E. J. *J. Chem. Phys.* **1995**, *103*, 9347−9354. (g) Rosa, A.; Baerends, E. J.; van Gisbergen, S. J. A.; van Lenthe, E.; Groeneveld, J. A.; Snijders, J. G. *J. Am. Chem. Soc.* **1999**, *121*, 10356−10365. (h) Casida, M. E.; Jamorski, C.; Casida, K. C.; Salahub, D. R. *J. Chem. Phys.* **1998**, *108*, 4439−4449.

(67) Wang, F.; Ziegler, T.; van Lenthe, E.; van Gisbergen, S.; Baerends, E. J. *J. Chem. Phys.* **2005**, 122.

(68) Manson, J.; Webster, C. E.; Pérez, L. M.; Hall, M. B.; http://www.chem.tamu.edu/jimp2/index.html.